

Realizing the Ideal Structure for Hybrid Photovoltaics by Directly Electrochemical Polymerizing Thiophene between ZnO Nanorods

Fei Wang^{1,*}, Zhigang Liu¹, Xiaofeng Zhang¹, Wenjia Zhang¹, Weifeng Guo¹, Wenli Lin¹, Qi Chen¹ and Zhijian Chen²

¹Beijing Institute of Spacecraft System Engineering, 100094, China

²State Key Laboratory for Mesoscopic Physics and Department of Physics, Peking University, Beijing, 100871, China

Abstract: A method to realize the ideal structure for Organic Photovoltaics (OPVs) was reported. Vertical aligned zinc oxide (ZnO) nanorods were hydro thermally grown on ITO or ITO/Poly(thiophene) (PTH) substrates as electron acceptor, and PTH was directly electrochemically polymerized between the ZnO nanorods as the electron donor. The interdigital structure between two semiconductors shall help the charge carriers to diffuse to electrodes much easier compared with disordered structures. Scanning Electron Microscope (SEM) was used to verify the nearly 100% inserting of PTH into the ZnO nanorods gaps. The method may define a new way to obtain other ideal structures and improve the performance of organic solar cells.

Keywords: Organic photovoltaics, ideal structure, ZnO nanorods, electrochemical polymerization.

1. INTRODUCTION

OPVs have been researched widely in the world for their low weight, flexible, and low cost properties [1-5]. When the concept of OPVs was firstly raised, P and n-type semiconductors were deposited as two separate films, so-called bilayer organic solar cell [6], and the afflatus might originate from the mature inorganic solar cells. But because of the different conductive mechanisms [7], organic semiconductors do not show as good electronic properties as inorganic semiconductors. Light induced electrons and holes usually bound together and form electron-hole pairs, named excitons; the excitons would transport from one molecule to another by jumping, and much energy would lose in this process. The diffusion length of excitons in organic semiconductors is about 10-20nm [8], and the excitons would decay when the transport distance is longer. As a result, thin p and n films are necessary for the bilayer OPVs; thus only a small amount of sunlight could be employed and much energy is missing. To balance the short diffusion length of excitons and the need of thicker films to absorb as much sunlight, researchers struggled and reported a new concept of OPVs-bulk heterojunction structure [9], and the Power Conversion Efficiency (PCE) was highly enhanced. For bulk heterojunction OPVs, bicontinuous way of two kinds of materials is necessary for good charge carrier transmission, which is usually achieved by thermal or solvent annealing [10]. For better

transmission of electrons and holes, another interdigital structure has been called out for many years [11], and researchers have been pursuing ways to realize the ideal structure. It is rather difficult to grow vertical aligned nanorods for most organic semiconductors and to insert another kind of organic material between the nanorods is even harder because of the flexible and amorphous molecular properties. Since inorganic materials usually possess tough characteristics, hybrid solar cells have been studied deeply: inorganic semiconductor is expected to be used as n-type materials and organic material is used as p-type one to absorb most of the sunlight [12-14]. ZnO, which is rather cheap and easy to form nanostructures, has been widely used in hybrid solar cells system [15-16]. Vertical aligned ZnO nanorods can be synthesized in many ways, such as Chemical Vapor Deposition (CVD) [17], hydrothermal synthesis [18], etc. P-type materials, such as poly(3-hexylthiophene) (P3HT), is spin-coated onto the nanorods commonly. But because of the big surface tension of the viscous polymer and small gaps between the nanorods, polymers are difficult to penetrate to the bottom of the nanorods, even annealing or long time soaking methods are applied. An incorporation of 22% rrP3HT was found to infiltrate the porous of TiO₂ by monitoring the ratio of carbon-ion signal-by means of secondary-ion mass spectrometry; without any treatment, the portion would be smaller [19].

In this article, we report a method to insert the organic semiconductor into the vertical aligned ZnO nanorods perfectly. ZnO nanorods were hydrothermally synthesized onto ITO or ITO/PTH substrate, and then

*Address correspondence to this author at the Beijing Institute of Spacecraft System Engineering, 100094, China; Tel: +86 10 68745810; Fax: +86 10 68745883; E-mail: wangfeiaa110@pku.edu.cn

PTH was directly electrochemically polymerized into the ZnO nanorods using thiophene as the monomer. SEM images verified the well penetrating result.

2. EXPERIMENTAL

2.1. Electrochemical Polymerization PTH Films

Electrochemical polymerization was carried out by using three-electrode system. ITO/glass was used as working electrode, and they were cleaned in deionized water, acetone and ethanol for 10mins respectively by using an Ultrasonic Clearing Machine. Thiophene without any substituent group was selected as monomer and it was dissolved in boron trifluoride ethylether (BFEE) as electrolyte, and the concentration of thiophene is 0.05mol/L (M). Helical platinum wire was used for counter electrode and saturated calomel electrode (SCE) was adopted as reference electrode. Nitrogen gas helped to eliminate the oxygen in the electrolyte for 15mins before polymerization. After the preparation, 1.3V direct voltage was added between the working and counter electrodes, and the distance between two electrodes was kept at 1cm. PTH film thickness was determined by the reaction time.

2.2. Fabrication of Devices

Several steps were proceeding in order. Firstly, a thin ZnO layer was deposited onto the PTH/ITO/glass with a Magnetron Sputtering System, which would act as a seed layer for the ZnO nanorods growth. Secondly, the samples were immersed into aqueous solution containing 25mM zinc acetate, 25mM hexamethylenetetramine (HMT), and 5mM poly-ethylenimine (PEI, $M_n=600$), and the reaction vessel was put into an oven at 92°C for 30min; different proportion $\text{In}(\text{NO}_3)_3$ was added in the solution to dope the ZnO nanorods. When taken out, the samples with ZnO vertical aligned nanorods were rinsed with water for several times to remove the remainders and then dried with nitrogen gas. Thirdly, they were put into the electrochemical pool, and acted as working electrode for the second time. Electrochemical polymerization was carried out for 10min to fill PTH into the gaps between ZnO nanorods. Some samples were transferred into the Oxygen Plasma Cleaning Machine to remove the PTH on the tips of ZnO nanorods, and others were not treated specially. Finally, 0.5nm LiF/300nm Al was deposited with a Thermal Evaporation System, and the film thickness was monitored by a Quartz Crystal.

The process flow was shown in Figure 1.

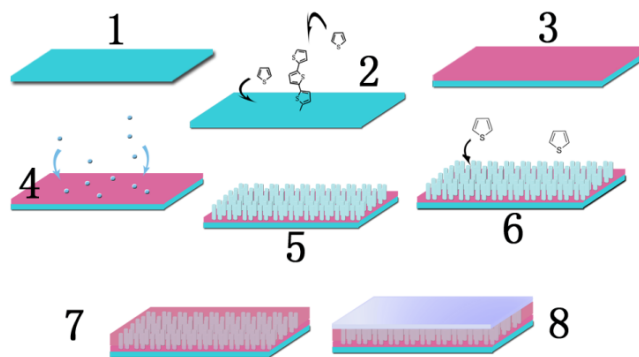


Figure 1: The process of fabricating the devices with a structure of ITO/PTH/ZnO:PTH/LiF/Al.

2.3. Measurement

The surface topography and characteristics of films were tested with SEM, atom force microscope (AFM), stylus profile (Veeco Dektak), x-ray diffraction (XRD), energy disperse spectrometer (EDS), and UV-visible spectrophotometer (Agilent 8453). The photovoltaic characteristics of the devices were measured using AM 1.5G simulated sunlight source (Newport 69911), and Keithley 2611 System Source Meter.

3. RESULTS AND DISCUSSION

For electrochemical polymerization, the electric current is rather sensitive to the voltage since the resistivity of electrolyte is small, and the film roughness is affected by the grow rate. In this study, we use 1.3V voltage for the PTH grow, and the grow rate is about 20nm/minute, meaning that it takes only 5mins to synthesize a 100nm film. When the voltage is lower, the roughness shows no differences, which is around 5~7nm in average, but the grow rate would decreased sharply. When the voltage is raised to 1.4V, the current increases an order of magnitude, and the surface roughness of films is enlarged to 15nm meanwhile. As the films generated on the ITO/glass substrate, a gray color, which implies the oxide state of the films could be seen on the surface; adding a reverse voltage of -1.3V could reduce the films, the doping of BF_4^- could be removed at the same time, and the color would recover to red as state of art [20].

The target structure is ITO/PTH/ZnO:PTH/LiF/Al. Here, ITO acts as anode; PTH is a p-type material; ZnO:PTH is a mixture layer and the key active layer; LiF/Al is the cathode. The first PTH layer shall no thicker than 20nm because of the short exciton diffusion length, and another reason is that, when this

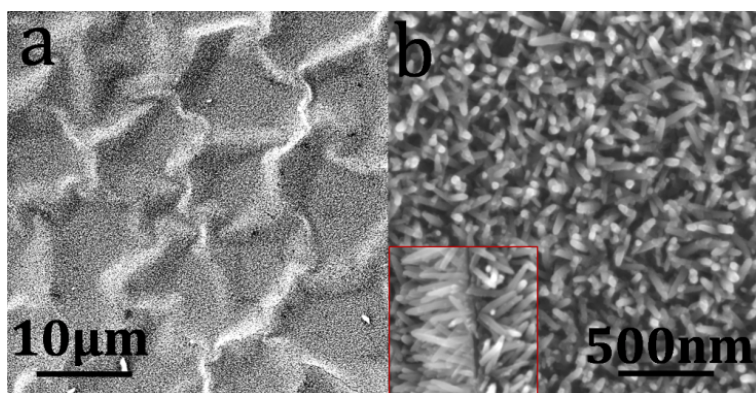


Figure 2: SEM images of ITO/PTH (thick)/ZnO. Inset: the ridge of the wrinkle.

Table 1: The Feasibility of Growing ZnO Nanorods on ITO, PTH/ITO, and Polymerizing PTH between the ZnO Nanorods Gaps on both Substrates

	1.1 nm ZnO seed layer	2.1 nm ZnO seed layer	4.3 nm ZnO seed layer	8.2 nm ZnO seed layer
Growing ZnO nanorods on ITO (30min growing time)	√	√	√	√
Electrochemical Polymerizing PTH between the nanorods gaps	√	√	√ non uniform	×
Growing ZnO nanorods on PTH/ITO (30min growing time)	√	√ (Figure 3)	√	√
Electrochemical Polymerizing PTH between the nanorods gaps	√	√ (Figure 3)	√ non uniform	×

layer is too thick, wrinkles appear after 30mins' bath in the aqueous solution, as shown in Figure 2.

Since ZnO does not show as good conductivity as ITO, when the ZnO layer is too thick, it is difficult to polymerize PTH onto the films, or the films would be rather non uniform; without the seed layer, it will be difficult to grow ZnO on the substrate directly. So the thickness of ZnO seed layer has to be determined. When using spin-coated method to form a p-type semiconductor, the seed layer is out of the question. Table 1 shows the feasibility of growing ZnO nanorods on ITO, PTH/ITO, and polymerizing PTH between the ZnO nanorods gaps on both substrates with different ZnO seed layers. It shows that 2nm is perfect enough for ZnO nanorods growth and PTH polymerization between the ZnO nanorods gaps.

To obtain good conductivity of ZnO, we doped In^{3+} during the hydrothermal process. Since the topographies of different of In^{3+} are nearly the same, only ZnO:In (2 at.%) is shown in the following figures. On PTH/ITO, ZnO nanorods as grown are vertical aligned to the substrate, without any difference from those on ITO itself. The length and width of the rods is around 200-300nm, and 50-60nm respectively, and the

gaps are on the same order of magnitude. That is to say, similar amount of PTH would be inserted into the gaps, and acts as electro-donor material. When PTH is polymerized, the top-view SEM image seems unclear and indistinct ZnO rods could be distinguished. Viewing from the cross section, shown in Figure 4, we could see clearly the whole process how PTH polymerizes between the gaps. When the polymerization time is short [Figures 4(a) and 4(c)], only a thin PTH layer on the bottom of the substrate could be seen on the top view; compared with the side view of ZnO nanorods itself (inset of Figure 3), PTH also appears on the body of ZnO. Since the worse conductivity of ZnO compared with ITO, the growth rate on the bottom of substrate and the ZnO bodies might be different. When growth time is longer [Figures 5(b) and 5(d)], the gaps are filled with PTH; simultaneously, small "hills" protrude above the film, and those must be the ZnO wearing a PTH cap layer. Qualitative to say, this cap layer would hinder the electrons transporting from ZnO to cathode. So, oxygen plasma is employed to remove a thin PTH cap layer in order that ZnO could form ohmic contact with Al cathode. Figure 5 compares the surface topographies before and after oxygen plasma is applied; the result is not that exciting since the surface turns uneven because of the different etching rate at

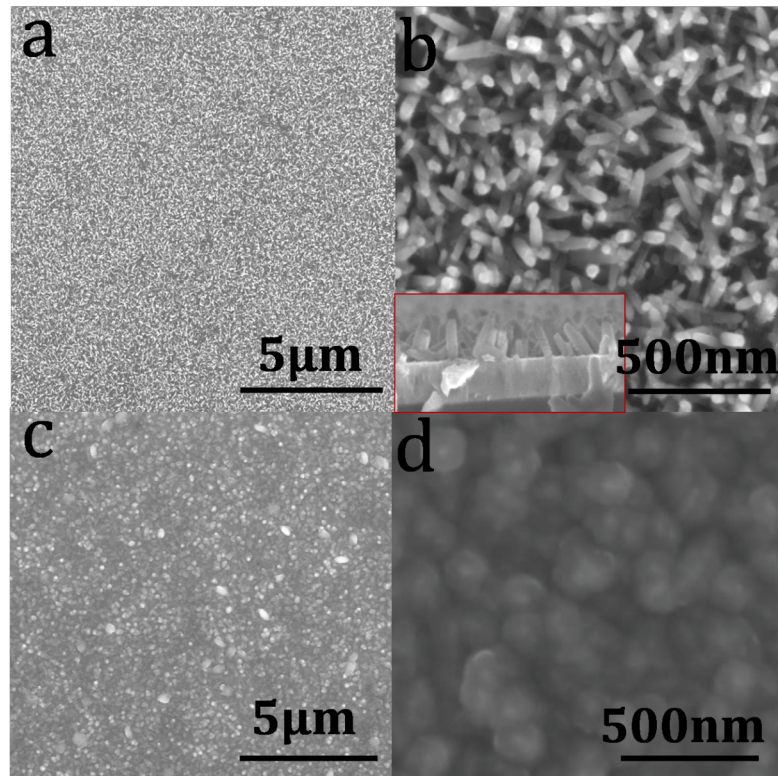


Figure 3: SEM images of ZnO/PTH (thin)/ITO. (a, b), and top-view SEM images of PTH/ZnO/PTH (thin)/ITO (c, d).

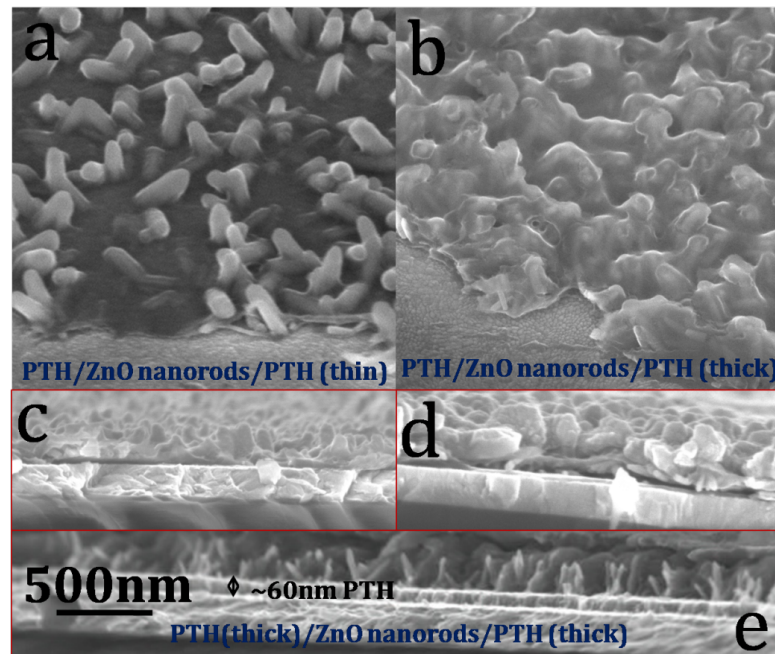


Figure 4: Side-view (a, b) and top-view (c, d, e) SEM images of PTH: ZnO/PTH/ITO; a, c show the situation when the growing time of upper PTH is short, and b, d with longer growing time; e is a image when the bottom PTH layer is as thick as 60nm. All of the images verify the perfect inserting of PTH into the ZnO nanorods gaps.

different site; the resulting defects may acts as recombination center in the photovoltaic devices.

The absorbance of the sample with a structure of ITO/PTH/ZnO:PTH is measured, shown in Figure 6.

The peaks at 373 and 478nm originate from ZnO and PTH respectively. And the absorbance edge is at ~620nm, which is similar with P3TH, meaning that PTH has nearly the same energy bandgap, ~2 eV. In order to research the doping effect of ZnO:In (x at.%), we

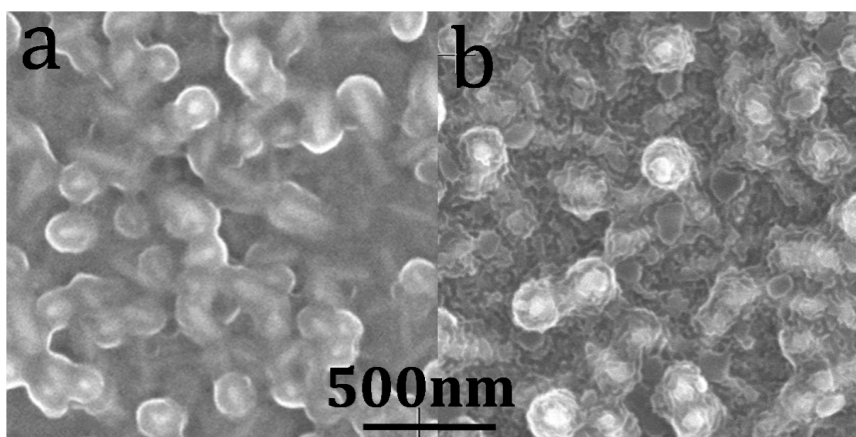


Figure 5: Surface topographies before, (a) and after, (b) the oxygen plasma treatment.

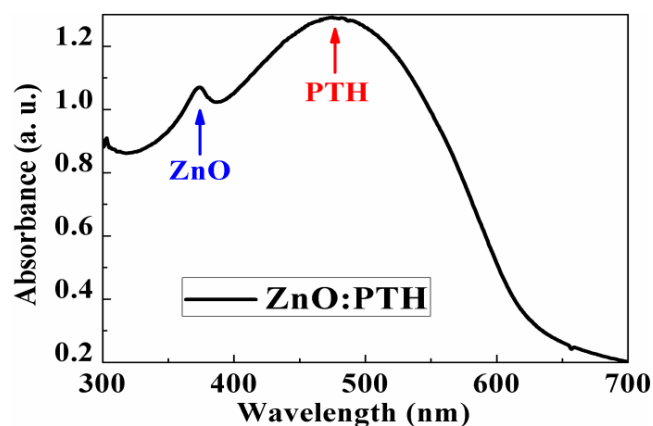


Figure 6: Absorbance of ZnO:PTH/ITO.

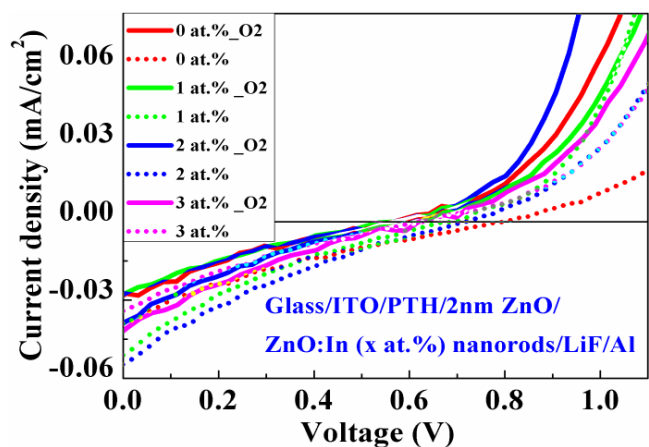


Figure 7: J - V curves of devices with different In^{3+} doping ratio.

fabricated different devices when $x=0, 1, 2, 3$, and the films with and without oxygen plasma etching process were also studied. J - V curves of the devices are shown in Figure 7, and the parameters are summarized in Table 2.

Open circuit voltages (V_{OC}) of the devices are among 0.57-0.77V. In organic solar cells, it is well known V_{OC} is mainly determined by the difference between the highest occupied molecular orbit (HOMO) of donor and the lowest unoccupied molecular orbit (LUMO), and affected by the Fermi level of two electrodes [21]. Here, the conduction band energy level (E_{CV}) of ZnO and the HOMO of PTH would play the main role. HOMO of PTH was tested with two methods: Cyclic Voltammetry (CV) with SCE as the reference electrode and Photoelectron Spectroscopy (PS). They show that the HOMO energy is -5.5 eV and -5.3 eV respectively for the same film; the difference may result from the different systemic error and a little change of the film surface when tested. The energy level difference between HOMO of PTH and E_{CV} of ZnO is about 0.9-1.1 eV, which would be the limit of V_{OC} , shown in Figure 8.

Actually, some of the energy would lose because of several reasons, such as non-perfect interface [22-23], and materials with large bulk resistivity, etc. The defects in ZnO, PTH or the interface would cause

Table 2: Parameters of the Devices

	x=0 _{O₂}	x=0	x=1 _{O₂}	x=1	x=2 _{O₂}	x=2	x=3 _{O₂}	x=3
V_{OC} (V)	0.57	0.77	0.57	0.71	0.57	0.71	0.62	0.63
J_{SC} (mA/cm ²)	0.032	0.040	0.030	0.053	0.042	0.056	0.045	0.036
FF	0.18	0.19	0.18	0.16	0.18	0.18	0.18	0.19
PCE (%)	0.0032	0.0059	0.0031	0.0061	0.0044	0.0073	0.0050	0.0043

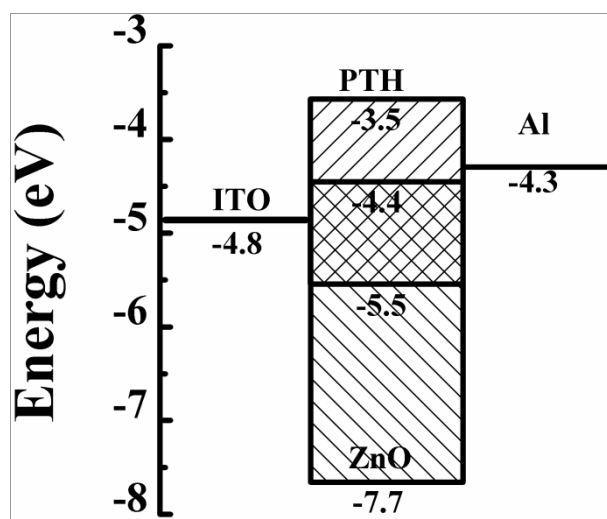


Figure 8: Energy level of materials in devices.

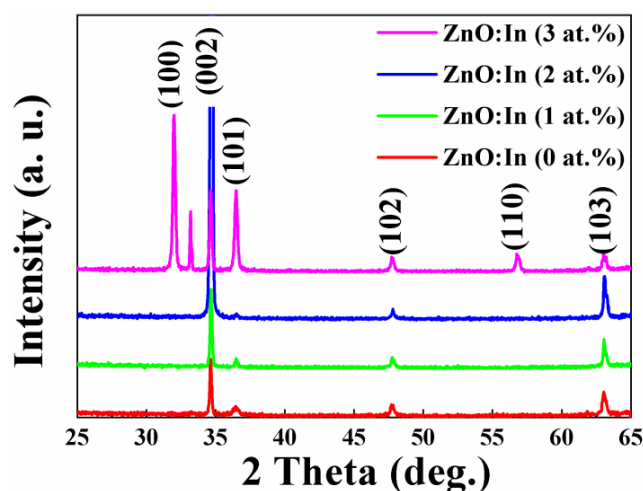


Figure 9: XRD data of ZnO:In (x at.%) grown on ITO.

recombination of electrons and holes, and fewer electrons and holes could reach the electrodes; so photo-electricity reduced rapidly. When organic material contacts with a metal and ohmic contact occurs, the Fermi level (E_F) would be pinned to an energy level of the organic material, which is called charge transfer state, and this energy level is usually lower than LUMO (for n-type semiconductor and a low E_F metal) and higher than HOMO (for p-type semiconductor and a high E_F metal); the charge transfer state is influenced by the surface states: the more the surface states are, the more energy will lose, in the name of smaller V_{OC} of OPVs [24-25]. Here, the large V_{OC} might result from the good crystal structure, larger mobility and less surface states of ZnO, and thus smaller loss from Fermi pinning at the interface of ZnO and Al compared with conventional devices based on P3HT:PCBM.

Compared with the devices treated by oxygen plasma, those without processing shows larger V_{OC} , which seems beyond our expectation. Actually, the answer may lie in the defects caused by the plasma; the defects at the junction would act as carrier recombination center, and that would result in lower photocurrent and V_{OC} [26-27].

For the devices with different In^{3+} doping ratio, short circuit current density (J_{SC}) and V_{OC} show no much difference. So, the conductivity of ZnO may be not the key point. The x-ray diffraction (XRD) data, shown in Figure 9, also indicates that the crystal lattices do not change with In^{3+} content (some other peaks for x=3 come from ZnO powder fallen on the substrate, which could be confirmed with SEM). In another respect, PTH films grown between the ZnO nanorods may possess tortile structure and shows smaller mobility compared with the films on plain substrates [28], and that might be the main problem. Thus, to optimize the steps may deduce the loss of photocurrent and improve the final PCE.

CONCLUSION

The interdigital structure of organic solar cells has been realized based on ZnO as electron acceptor and electrochemically polymerized PTH as electron donor. SEM images confirm the structure. Compared with conventional organic OPVs, the devices here posses larger V_{OC} which might be caused by the few surface states of ZnO and thus little energy loss when ZnO contacts with Al. The method may lead a way to achieve some other ideal structures and improve the charge carrier transport from active layer of OPVs to the corresponding electrode.

ACKNOWLEDGEMENT

This work was supported by the National Natural Science Foundation of China under grant Nos. 10934001, 60878019 and 10821062, and the National Basic Research Program under grant Nos. 2007CB307000 and 2009CB930504.

REFERENCES

- [1] Agrawal N, Ansari Mohd Z, Majumdar A, Gahlot R and Khare N. Sol Energy Mat Sol Cells 2016; 157: 960-965. <https://doi.org/10.1016/j.solmat.2016.07.040>
- [2] Chao Y, Chuang C, Hsu H. Sol Energy Mat Sol Cells 2016; 157: 666-675. <https://doi.org/10.1016/j.solmat.2016.07.041>
- [3] Keru G, Ndungu PG, Nyamori VO. Int J Energy Res 2014; 38: 1635-1653. <https://doi.org/10.1002/er.3194>

- [4] Goldschmidt JC and Fischer S. *Adv Opt Mater* 2015; 3: 510-535.
<https://doi.org/10.1002/adom.201500024>
- [5] Kulshreshtha C, Choi JW, Kim J, Jeon WS, Suh MC, Park Y, *et al.* *Appl Phys Lett* 2011; 99: 023308.
<https://doi.org/10.1063/1.3610962>
- [6] Tang CW. *Appl Phys Lett* 1986; 48: 183-185.
<https://doi.org/10.1063/1.96937>
- [7] Saito G and Yoshida Y. *Bull Chem Soc Jpn* 2007; 80: 1-137.
<https://doi.org/10.1246/bcsj.80.1>
- [8] Winder C and Sariciftci NS. *J Mater Chem* 2004; 14: 1077-1086.
<https://doi.org/10.1039/b306630d>
- [9] Ma W, Yang C, Gong X, Lee K and Heeger AJ. *Adv Funct Mater* 2005; 15: 1617-1622.
<https://doi.org/10.1002/adfm.200500211>
- [10] Yu G, Gao J, Hummelen JC, Wudl F and Heeger AJ. *Science* 1995; 270: 1789-1791.
<https://doi.org/10.1126/science.270.5243.1789>
- [11] Peet J, Kim JY, Coates NE, Ma WL, Moses D, Heeger AJ, *et al.* *Nat Mater* 2007; 6: 497-500.
<https://doi.org/10.1038/nmat1928>
- [12] Günes S, Neugebauer H and Sariciftci NS. *Chem Rev* 2007; 107: 1324-1338.
<https://doi.org/10.1021/cr050149z>
- [13] Qin Y, Wang X and Wang Z. *Nature* 2008; 451: 809-814.
<https://doi.org/10.1038/nature06601>
- [14] Shu Q, Wei J, Wang K, Zhu H, Li Z, Jia Yi, *et al.* *Nano Lett* 2009; 9, 4338-4342.
<https://doi.org/10.1021/nl902581k>
- [15] Huynh WU, Dittmer JJ and Alivisatos AP. *Science* 2002; 295: 2425-2427.
<https://doi.org/10.1126/science.1069156>
- [16] Xu C, Wang X, Lin Wang Z. *J Am Chem Soc* 2009; 131: 5866-5872.
<https://doi.org/10.1021/ja810158x>
- [17] Oosterhout SD, Koster LJA, Bavel SSV, Loos J, Stenzel O, Thiedmann R, *et al.* *Adv Energy Mater* 2011; 1: 90-96.
<https://doi.org/10.1002/aenm.201000022>
- [18] Wu J and Liu S. *Adv Mater* 2002; 14: 215-218.
[https://doi.org/10.1002/1521-4095\(20020205\)14:3<215::AID-ADMA215>3.0.CO;2-J](https://doi.org/10.1002/1521-4095(20020205)14:3<215::AID-ADMA215>3.0.CO;2-J)
- [19] Law M, Greene LE, Johnson JC, Saykally R and Yang P. *Nat Mater* 2005; 4: 455-459.
<https://doi.org/10.1038/nmat1387>
- [20] Bartholomew GP and Heeger AJ. *Adv Funct Mater* 2005; 15: 677-682.
<https://doi.org/10.1002/adfm.200400277>
- [21] Fan B, Wang P, Wang L and Shi G. *Sol Energy Mat Sol Cells* 2006; 90: 3547-3556.
<https://doi.org/10.1016/j.solmat.2006.06.042>
- [22] Scharber MC, Mühlbacher D, Koppe M, Denk P, Waldauf C, Heeger AJ, *et al.* *Adv Mater* 2006; 18: 789-794.
<https://doi.org/10.1002/adma.200501717>
- [23] Potscavage WJ, Sharma JRA and Kippelen B. *Accounts Chem Res* 2009; 42: 1758-1767.
<https://doi.org/10.1021/ar900139v>
- [24] Treat ND, Campos LM, Dimitriou MD, Ma B, Chabynyc ML, Hawker CJ. *Adv Mater* 2010; 22: 4982-4986.
<https://doi.org/10.1002/adma.201001967>
- [25] Braun S, Salaneck WR and Fahlman M. *Adv Mater* 2009; 21: 1450-1472.
<https://doi.org/10.1002/adma.200802893>
- [26] Steim R, Kogler FR and Brabec CJ. *J Mater Chem* 2010; 20: 2499-2512.
<https://doi.org/10.1039/b921624c>
- [27] Krüger J, Plass R, Cevey L, Piccirelli M and Grätzel M. *Appl Phys Lett* 2001; 79: 2085-2087.
<https://doi.org/10.1063/1.1406148>
- [28] Conings B, Baeten L, Boyen HG, Spoltore D, D'Haen J and Grieten L. *J Phys Chem C* 2011; 115: 16695-16700.
<https://doi.org/10.1021/jp203699h>

Received on 15-10-2016

Accepted on 05-01-2017

Published on 23-10-2017

DOI: <https://doi.org/10.12974/2311-8717.2017.05.01.2>© 2017 Wang *et al.*; Licensee Savvy Science Publisher.

This is an open access article licensed under the terms of the Creative Commons Attribution Non-Commercial License (<http://creativecommons.org/licenses/by-nc/3.0/>) which permits unrestricted, non-commercial use, distribution and reproduction in any medium, provided the work is properly cited.